Stochastic Seasonal Planning of DG-Based Smart Grid and Energy Hub by Considering Demand Response Program and Environmental Impacts

Narges S. Ghiasi
Holcombe Department of Electrical and Computer Engineering
Clemson University
Charleston, United States
nghiasi@clemson.edu

Seyyed Mohammad Sadegh Ghiasi*
Department of Electrical Engineering
Ahvaz Branch
Islamic Azad University
Ahvaz, Iran
smsghiasi@aut.ac.ir

Ramtin Hadidi
Holcombe Department of Electrical and Computer Engineering
Clemson University
Charleston, United States
rhadidi@clemson.edu

Abstract— **This paper presents a stochastic optimization program for multi-objective cost and environmental pollution optimization in a network over a one-year time horizon. In this context, the system operator, in addition to planning equipment utilization, mitigates the effects of existing fluctuations in the uncertain input parameters by employing demand response programs. Random functions are used to model the oscillatory behavior of wind turbine speed. Furthermore, planning is performed for different seasons of the year to examine the sensitivity of the obtained response to weather conditions. To simulate the proposed model, a mixed-integer linear programming (MILP) approach is employed, and the GAMS software is used to solve it. Considering uncertainty in wind turbine generation, the proposed model is applied to a test microgrid consisting of multiple energy carriers. Simulation results demonstrate the impact of demand response programs while increasing the cost of planning due to the consideration of uncertainty in the system.**

Keywords— energy hub, demand response, multi-objective optimization, stochastic programming.

I. INTRODUCTION

With the restructuring of the electricity industry, networks consisting of multiple energy carriers have entered this field, referred to as energy hubs. A microgrid comprising multiple energy carriers includes a set of small-scale consumers and producers that mainly interact with the distribution network at a low voltage level. In this microgrid, not only electrical energy but also other energy carriers exist alongside consumers and suppliers. For example, thermal loads, cooling, heating, and even natural gas-consuming equipment may exist in a microgrid consisting of multiple energy carriers. In addition to the mentioned equipment, energy storage systems can also serve as another energy source [1].

From a research perspective, the topic of planning and operating a microgrid consisting of multiple energy carriers involves both long-term and short-term aspects. In the long-term phase, the primary objective is to determine the optimal capacity of the desired equipment for investment, while in the short-term phase, the goal is to determine the optimal operating point for each of the equipment in the energy hubs. Additionally, proper interaction with the electric power distribution network and gas distribution network for purchasing energy from or selling it to the upstream network is a significant part of operating a microgrid consisting of multiple energy carriers [1].

In recent years, the optimal operation of multi-energy systems, or energy hub systems, has been one of the key topics in power system planning [2]. In such conditions, different energy sources, such as combined heat and power units, are utilized to enhance the efficiency of various energy carriers [3]. Furthermore, thermal energy sources in the generation cycle, such as steam boilers, can be optimally utilized to meet thermal demand [4]. In addition to the mentioned renewable energy sources, renewable generation units can be combined in energy hub systems to answer various load demands [1]. It should be noted that the use of thermal sources and fossil fuel-consuming devices in energy hub systems has turned the issue of pollution emissions into a significant challenge for system operators [5].

In recent years, extensive researches have been carried out regarding energy-related topics. A mathematical model for optimizing the exploitation of an intelligent energy network using energy hubs is presented in [6]. This model utilizes hydrogen as an energy carrier and aims to investigate the advantages of hydrogen production in a smart energy grid. The placement of power plants in an energy system connected to natural gas and electricity, in the form of conversion hubs, including converters for electricity-to-gas and renewable energy sources, is examined in [7]. References [8] and [9] present a new model for energy hubs considering hydrogen as an energy carrier within the hubs. Reference [10] investigates the optimization of a multi-carrier energy hub system and determines suitable investments for generation units, transmission, and furnaces. Considering natural gas and the simultaneous production of electricity and heat, reference [11] models a residential building as an energy hub, due to various heat and electrical appliances. Daily energy consumption in regional buildings has been optimized using the concept of energy hubs in reference [12].

Reference [13] examines the optimal operation of multi-carrier energy systems in the presence of wind farms, thermal and electrical storage systems, the electricity market, and the heat energy market. The impact of distributed generation, uncertainties, demand, price, and wind on the operational costs and reliability of energy hubs is studied in reference [14].

Some researchers have investigated various models for planning and operating energy systems, some of which are mentioned in the following. In [15], the reliability of an electric energy system without considering interactions with other energy carriers is presented using a linear model of AC load flow equations. In [16], by employing DC load flow equations in the power grid and a detailed model of the natural gas transmission network, the coordination between electricity and natural gas networks in the optimal operation of gas-fired power generation units to enhance the performance of energy systems is studied. A model is

presented in [17] to examine the energy system's security in response to demand and the effects of the natural gas network on the optimal operation of electricity and natural gas systems without considering their mutual interaction. Various models of energy carrier integration for the optimal operation of multi-carrier energy systems are presented in [18-21]. To improve the speed of load distribution problem-solving in the power grid, a linear model of optimal energy distribution in electricity and natural gas networks using the concept of energy hubs is introduced in [18]. In [19], a model is proposed for the optimal operation of multi-carrier energy systems by utilizing renewable energy sources, combined heat and power units, and the behavior of electric vehicle owners in providing storage services. A resilient optimization method for optimal energy management in multi-carrier systems with uncertainties in price, energy demand, and equipment efficiency within energy hubs is presented in [20].

Although these systems are capable of providing various services such as electricity, heating, and cooling, their emission of pollution is a challenging issue. Since improving each of the cost and pollution functions has a negative impact on the other function, it is necessary to find a solution that creates a balance. In this paper, a multi-objective stochastic approach is presented to optimize the cost and environmental pollution during the planning horizon of one year. In these conditions, the system operator, in addition to planning the operation of equipment, will mitigate the effects of existing fluctuations in the system's input parameters using demand response programs. Random functions are used to model the oscillatory behavior of wind turbine speed. Additionally, to examine the sensitivity of the obtained response to weather conditions, the planning is modeled for each year in four different seasons. The proposed model is implemented on a microgrid consisting of multiple energy carriers, and comparative results are provided to validate the effectiveness of the proposed method.

Section 2 of this article addresses the formulation of the energy hub problem. In section 3, a case study is presented to investigate the effectiveness of the proposed method, while the results are presented in section 4.

II. Energy Hub Problem Formulation

The examined energy hub structure in this paper is illustrated in Fig. 1. The energy inputs consist of four systems: water, electricity, gas, and wind energy, and the system accommodates various electrical, thermal, and gas loads. The equipment in the hub is divided into two categories: thermal and electrical. They include a boiler, a combined heat and power (CHP) generation unit, a thermal energy storage system (TEES), and an electrical energy storage system (EESS), respectively. The input electricity is supplied to the energy hub from the grid and wind power plant through transformers and converters. It should be noted that the main programmable loads in this energy hub are electrical and thermal loads. Furthermore, by adding the cooling load, three devices of the heater, absorption chiller (AC), and electrical heat pump (EHP), are considered in the proposed model.

To solve the multi-objective problem, the Epsilon Constraint method is utilized. Considering the cooling load and the one-year planning horizon, four types of seasonal load curves are considered for electrical, heating, and cooling loads. Uncertainty is also taken into account in the planning.

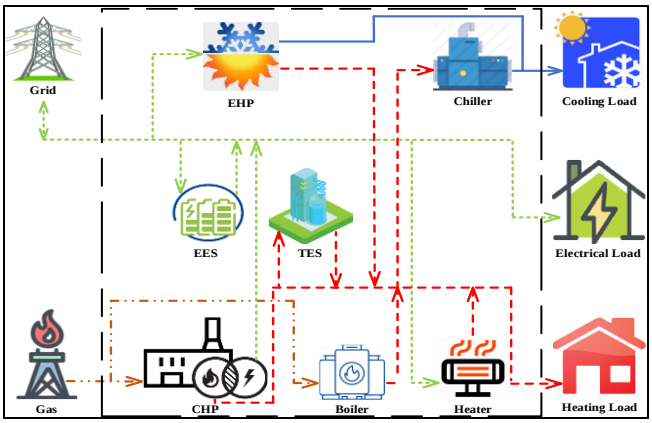

Fig. 1. Studied energy hub system

A. Optimization Objective Functions

The main model of the energy hub in Fig. 1 is formulated as a linear model that can be solved using the CPLEX solver. In this study, two objective functions are considered: minimizing the planning cost and minimizing the emission pollution. The operating cost includes the cost of purchasing electricity from the grid, the cost of using wind energy, the cost of using electrical and thermal energy storage systems, the cost of using demand response programs, profit (or cost) from energy sales (or purchases), water consumption cost, and gas consumption cost by the CHP unit and boiler, as shown in the following equation:

$$\Phi_1 = cost = \sum_t^H \lambda_t^e P_t^e + \lambda^{wi} P_t^{wi} + \lambda_s^e \left(P_t^{ch,e} + P_t^{dis,e}\right) + \lambda^{DR}\left(P_t^{e,shdo} + P_t^{e,shup}\right) + \lambda_t^e \left(P_t^{ch,e} - P_t^{dis,e}\right) + \lambda^g g_t^{CHP} + \lambda^g g_t^B + \lambda_s^h \left(P_t^{ch,h} + P_t^{dis,h}\right) \quad (1)$$

Furthermore, the overall system pollution, which includes pollution from CHP, boiler, gas consumption, and electricity consumption, is considered according to the following equation:

$$Min\ \Phi_2 = Em = EF^{CHP}.g_t^{CHP} + EF^B.g_t^B + EF^L.g_t^L + EF^{NET}.p_t^{NET} \quad (2)$$

B. Constraints

Considering the energy hub and its associated equipment, the imposed constraints can be broadly categorized into four main categories: electrical constraints, thermal constraints, cooling constraints, and gas-related constraints. The following equation represents the electrical energy balance modeled in the energy hub.

$$p_t^{el} + p_t^{shup} - p_t^{shdo} = A^{Net}.\eta_{ee}^T.p_t^e + A^{WIND}.\eta_{ee}^{CON}.p_t^{wi} + A^{CHP}.\eta_{ge}^{CHP}.g_t^{CHP} + \left(p_t^{dis,e} - p_t^{ch,e}\right) - p_t^{HP,e} - p_t^{EC,e} \quad (3)$$

Furthermore, the limit of purchasing electrical power constraint due to the transformers and transmission lines is represented by the following equations:

$$p_e^{min} \le p_t^e \le p_e^{max} \quad (4)$$

$$\eta_{ee}^T.p_t^e \le p_e^T \quad (5)$$

The power generation of the wind turbine is taken into account based on the wind speed using the following equation:

$$p_t^{wi} = \begin{cases} 0 & w < w_{ci} \\ p_r & w_{ci} \le w \le w_r \\ p_r(z - y.w(t) + x.w^2(t)) & w_r \le w \le w_{co} \\ 0 & w \ge w_{co} \end{cases} \quad (6)$$

Equations (7) to (10) define the constraints related to the energy storage in the battery, considering the charging and discharging efficiency, minimum and maximum battery charge levels, system losses based on the battery charge level, and minimum and maximum battery charge rates.

$$C_t^{st,e} = C_{t-1}^{st,e} + P_t^{ch,e}.\eta_{ch}^e - P_t^{dis,e}/\eta_{dis}^e - P_t^{loss} \quad (7)$$

$$\alpha_{min}^e.C_c^{st,e} \le C_t^{st,e} \le \alpha_{max}^e.C_c^{st,e} \quad (8)$$

$$P_t^{loss,e} = \alpha_{loss}^e.C_c^{st,e} \quad (9)$$

$$\frac{\alpha_{min}^e.C_c^{st,e}.I_t^{ch}}{\eta_{ch}^e} \le p_t^{ch,e} \le \frac{\alpha_{max}^e.C_c^{st,e}.I_t^{ch}}{\eta_{ch}^e} \quad (10)$$

The set of (11) to (14) represents the status of transferable loads in the demand response program, the control of the rate of load growth or reduction within a time step to make a balance in the transferred loads over the entire time interval.

$$P_t^{el,DRP} = P_t^{el} + P_t^{shup,e} - P_t^{shdo} \quad (11)$$

$$0 \le P_t^{shup,e} \le LPF^{shup,e}.P_t^l.I_t^{shup,e} \quad (12)$$

$$0 \le P_t^{shdo,e} \le LPF^{shdo,e}.P_t^l.I_t^{shdo,e} \quad (13)$$

$$\sum_t^H P_t^{shup,e} = \sum_t^H P_t^{shdo,e} \quad (14)$$

Equations (15) to (19) pertains, respectively, to the thermal energy balance in the energy hub, the level of energy stored in the thermal storage, the losses of the thermal storage system, the limitation on the level of stored energy, and the hourly charging and discharging rates.

$$P_t^h = \eta_{gh}^B.g_t^B + A^{CHP}.\eta_{gh}^{CHP}.g_t^{CHP} + \left(p_t^{dis,h} - p_t^{ch,h}\right) + p_t^{HP,c}.p_t^{AC,h} \quad (15)$$

$$C_t^{st,h} = C_{t-1}^{st,h} + p_t^{ch,h}.\eta_{ch}^h - p_t^{dis,h}/\eta_{dis}^h - p_t^{loss,h} \quad (16)$$

$$P_t^{loss,h} = \alpha_{loss}^h.C_c^{st,h} \quad (17)$$

$$\frac{\alpha_{min}^h.C_c^{st,h}.I_t^{ch,h}}{\eta_{ch}^h} \le p_t^{ch,h} \le \frac{\alpha_{max}^h.C_c^{st,h}.I_t^{ch,h}}{\eta_{ch}^h} \quad (18)$$

$$\alpha_{min}^h C_c^{st,h} I_t^{dis,h} \eta_{dis}^h \le p_t^{dis,h} \le \alpha_{max}^h C_c^{st,h} I_t^{dis,h} \eta_{dis}^h \quad (19)$$

Since cooling loads also exist in the energy hub, corresponding cooling constraints need to be considered. Therefore, constraints related to achieving thermal balance, the absorption chiller capacity constraint, the heat pump capacity constraint, cooling limitations, and the heat production limitation of the heat pump are incorporated according to the following equations:

$$P_t^c = \eta_{hc}^{AC}.p_t^{AC,h} + p^{HP,c} + \eta_{hc}^{EC}.p_t^{EC,e} \quad (20)$$

$$\eta_{hc}^{AC}.p_t^{AC,h} \le p_c^{AC} \quad (21)$$

$$p_t^{HP,e} \le p_c^{HP} \quad (22)$$

$$p_t^{HP,c} \le \eta_{ec}^{HP}.p_t^{HP,e} \quad (23)$$

$$p_t^{HP,h} \le \eta_{ec}^{HP}.p_t^{HP,e} \quad (24)$$

Having the gas energy carrier in the investigated energy hub, its constraints are as follows:

$$g_t^{net} = g_t^B + g_t^{CHP} + g_t^l \quad (25)$$

$$g_{min}^{net} \le g_t^{net} \le g_{max}^{net} \quad (26)$$

$$\eta_{ge}^{CHP}.g_t^{CHP} \le p_c^{CHP} \quad (27)$$

$$\eta_{gh}^B.g_t^B \le p_c^B \quad (28)$$

Where these equations represent the constraints on total gas consumption in the energy hub, the constraint on gas consumption limitation, and the capacity constraints of using the two devices, CHP and boiler.

III. Case Study

Based on the network shown in Fig. 1, the data used for the energy hub includes electrical load, heating load, cooling load, electricity energy prices, and wind speed. The values for all these variables, except for wind speed, are displayed in Fig. 2 to Fig. 5.

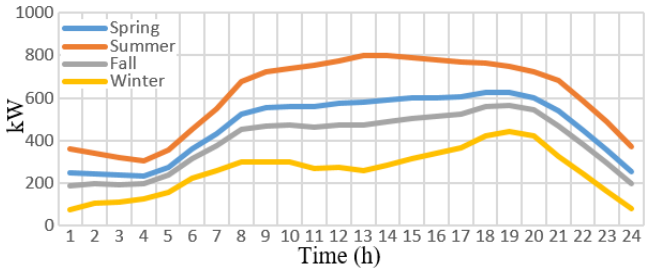

Fig. 2. Electrical Load profile

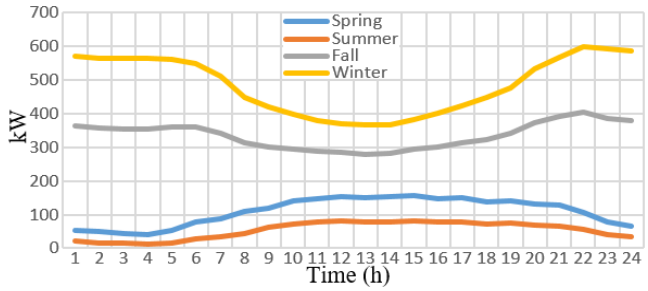

Fig. 3. Thermal load profile

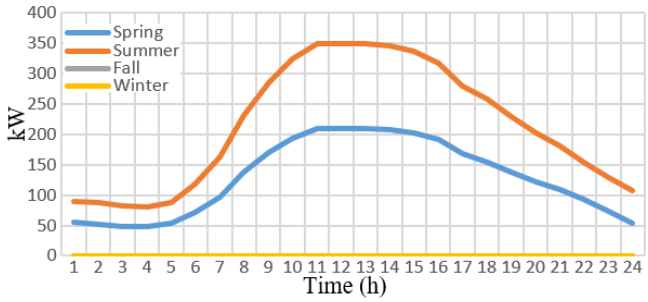

Fig. 4. Cooling load profile

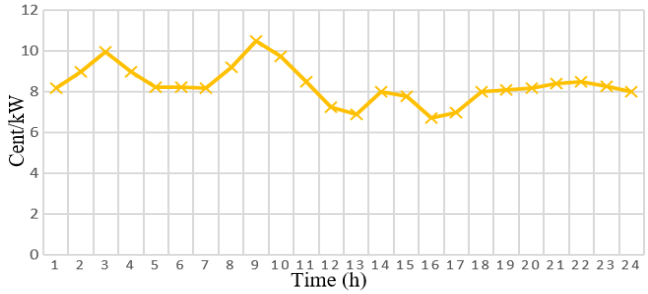

Fig. 5. Price by hour

In order to incorporate the stochastic nature of wind speed, it is necessary to consider the uncertainty associated with it. In this paper, creating and analyzing different scenarios is responsible to address this issue. To do so, a series of base wind speed data for each season, as shown in Fig. 6, is initially utilized.

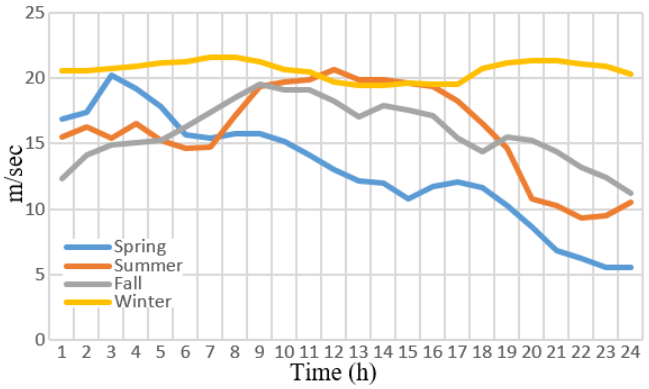

Fig. 6. Wind speed profile

Then, assuming a maximum 20% variation in these data, a vector with 9 random values ranging from +0.2 to -0.2 is created. By considering the base state, a total of 10 different scenarios, as presented in Table I, are formed.

TABLE I. MAXIMUM WIND SPEED CHANGE IN EACH SCENARIO COMPARED TO THE BASE CASE

Scenario No.	S1	S2	S3	S4	S5	S6	S7	S8	S9	S10
Maximum deviation	00.00	+0.05	-0.06	+0.08	-0.10	+0.12	-0.13	+0.16	-0.17	+0.18

Then, for each scenario, 24 random numbers are generated in such a way that their maximum deviation from the number 1 corresponds to the scenario coefficient given in Table I. By multiplying these 24 random numbers with the base state values, the wind speed values for the 10 scenarios are created for each season. As an example, Table II represents the coefficients used to generate the 10 wind speed scenarios for the spring season using this method.

TABLE II. TWENTY FOUR HOUR COEFFICIENTS FOR TEN WIND SPEED SCENARIOS

Scenario No. / Hour	1	2	3	4	5	6	7	8	9	10
1	1.000	1.040	0.973	1.026	0.905	1.054	0.950	1.040	0.833	1.040
2	1.000	1.048	0.949	1.044	0.901	1.105	0.952	1.071	0.997	1.163
3	1.000	1.024	0.952	1.029	0.908	1.036	0.884	1.063	0.938	1.169
4	1.000	1.047	0.986	1.039	0.922	1.104	0.985	1.104	0.964	1.073
5	1.000	1.040	0.947	1.002	0.906	1.072	0.899	1.075	0.885	1.161
6	1.000	1.025	0.986	1.054	0.938	1.053	0.944	1.127	0.941	1.157
7	1.000	1.037	0.985	1.022	0.922	1.032	0.930	1.104	0.881	1.093
8	1.000	1.031	0.969	1.014	0.907	1.057	0.957	1.067	0.876	1.054
9	1.000	1.038	0.965	1.043	0.996	1.051	0.912	1.080	0.940	1.104
10	1.000	1.048	0.961	1.063	0.966	1.002	0.920	1.102	0.986	1.114
11	1.000	1.021	0.973	1.059	0.996	1.020	0.941	1.151	0.903	1.071
12	1.000	1.028	0.962	1.004	0.910	1.073	0.967	1.077	0.985	1.116
13	1.000	1.018	0.960	1.035	0.905	1.071	0.957	1.150	0.839	1.064
14	1.000	1.003	0.950	1.033	0.995	1.003	0.973	1.076	0.879	1.152
15	1.000	1.049	0.949	1.034	0.970	1.049	0.973	1.060	0.899	1.169
16	1.000	1.036	0.964	1.003	0.961	1.025	0.955	1.091	0.839	1.014
17	1.000	1.025	0.962	1.006	0.940	1.048	0.890	1.060	0.993	1.113
18	1.000	1.024	0.981	1.030	0.995	1.099	0.974	1.027	0.929	1.061
19	1.000	1.044	0.995	1.071	0.976	1.050	0.876	1.023	0.907	1.049
20	1.000	1.048	0.950	1.079	0.981	1.007	0.922	1.130	0.876	1.030
21	1.000	1.028	0.947	1.035	0.917	1.052	0.879	1.025	0.964	1.125
22	1.000	1.014	0.983	1.001	0.921	1.104	0.886	1.071	0.986	1.064
23	1.000	1.009	0.977	1.038	0.920	1.061	0.871	1.104	0.865	1.081
24	1.000	1.037	0.944	1.075	0.923	1.109	0.901	1.137	0.884	1.007

The parameters of the wind turbine according to (6) are provided in Table III, and the efficiencies of the equipment used in the simulation are given in Table IV.

TABLE III. WIND TURBINE'S PARAMETERS

Parameter	Pr (kW)	CutIn Speed (m/s)	Rated Speed (m/s)	CutOut Speed (m/s)	x	y	z
Value	400	4	10	22	0.07	0.01	0.03

TABLE IV. EQUIPMENT EFFICIENCY

System	Operation	Value (%)
Boiler	Gas to Heat	85
Absorption chiller	Heat to Cooling	85
CHP	Gas to Electricity	40
	Gas to Heat	35
Heat Pump	Electricity to cooling	85
	Electricity to Heat	85
Heat Storage	Charging	90
	Discharging	90
Electrical Storage	Charging	90
	Discharging	90

The given power for the equipment in the simulation are shown in Table V.

TABLE V. EQUIPMENT CAPACITY

System	Parameter	Value
Heat Storage	Capacity (kW)	200
Electrical Storage	Capacity (kW)	300
CHP	Capacity (kW)	800
Absorption chiller	Capacity (kW)	350
Heat Pump	Capacity (kW)	150
Transformer	Capacity (kW)	800
Upstream Feeder	Import (kW)	1000
	Export (kW)	1000
Boiler	Capacity (kW)	800
	Max Water Consumption (kW)	1000
	Max Gas Consumption (kW)	1800

It should be noted that the emission factors for the boiler, upstream network, and CHP are 0.38 kg/kWh, 0.58 kg/kWh, and 0.36 kg/kWh, respectively. The gas and water purchase costs are considered as 6 cent/kWh and 4 cent/kWh, respectively.

IV. SIMULATION RESULTS

In the conducted simulations, the Epsilon Constraint method was used, and to examine the impact of the demand response program, simulations were performed in two scenarios: with and without the demand response program. The results of these scenarios were compared to each other. Additionally, to assess the impact of uncertainty in annual planning, this comparison was carried out once under deterministic conditions and once under uncertainty.

Firstly, network planning was performed for a one-year period, considering different seasons. The boundary values for the Epsilon Constraint method are shown in Table VI. As it can be seen, the optimal value in the presence and absence of the demand response program is located at points 4 and 3, respectively.

TABLE VI. PARETO FRONT USING EPSILON CONSTRAINT METHOD IN DETERMINISTIC PROGRAMMING

	No.	Cost	Emission	φ1	φ2	φmin
Without DRP	1	353076.2	1684423	0.002	1	0.002
	2	321319	1696194	0.537	0.9	0.537
	3	313381.7	1707966	0.671	0.8	0.671
	4	**309294.6**	**1719737**	**0.74**	**0.7**	**0.7**
	5	305207.6	1731509	0.809	0.6	0.6
	6	301120.5	1743280	0.878	0.5	0.5
	7	297528.7	1755052	0.938	0.4	0.4
	8	296496.3	1766823	0.955	0.3	0.3
	9	295613.7	1778595	0.97	0.2	0.2
	10	294731.1	1790366	0.985	0.1	0.1
	11	293848.4	1802138	1	0	0
	No.	**Cost**	**Emission**	**φ1**	**φ2**	**φmin**
With DRP	1	339086.9	1676270	0.16	1	0.16
	2	311961.4	1684902	0.59	0.9	0.59
	3	**301187.3**	**1693535**	**0.76**	**0.8**	**0.76**
	4	297580.8	1702168	0.817	0.7	0.7
	5	294583.5	1710800	0.865	0.6	0.6
	6	291586.2	1719433	0.912	0.5	0.5
	7	288899.6	1728066	0.955	0.4	0.4
	8	288005.3	1736698	0.969	0.3	0.3
	9	287358	1745331	0.979	0.2	0.2
	10	286710.7	1753964	0.99	0.1	0.1
	11	286063.4	1762596	1	0	0

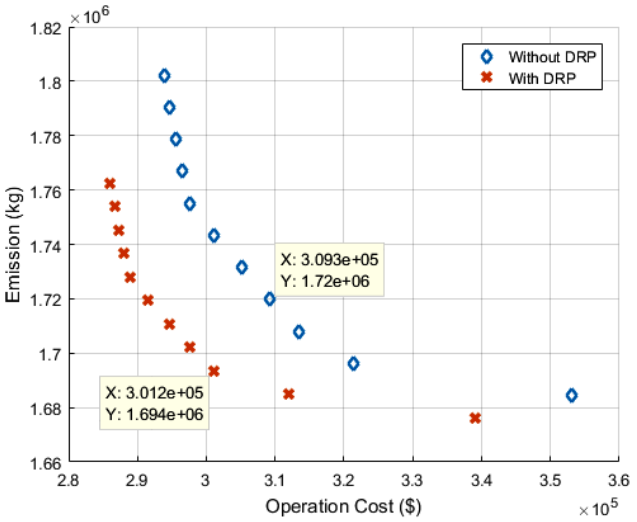

Fig. 7. Pareto front using Epsilon Constraint method in deterministic programming

TABLE VII. PARETO FRONT USING EPSILON CONSTRAINT METHOD IN STOCHASTIC PROGRAMMING

	No.	Cost	Emission	φ1	φ2	φmin
Without DRP	1	369629.7	1773541	0.006	1	0.006
	2	337529.5	1786539	0.541	0.9	0.541
	3	330331.1	1799538	0.661	0.8	0.661
	4	**325817.9**	**1812537**	**0.736**	**0.7**	**0.7**
	5	321304.8	1825536	0.812	0.6	0.6
	6	316791.6	1838534	0.887	0.5	0.5
	7	313961	1851533	0.934	0.4	0.4
	8	312928.3	1864532	0.951	0.3	0.3
	9	311960.7	1877531	0.967	0.2	0.2
	10	310986	1890529	0.984	0.1	0.1
	11	310011.4	1903528	1	0	0
	No.	**Cost**	**Emission**	**φ1**	**φ2**	**φmin**
With DRP	1	356140	1766706	0.171	1	0.171
	2	327653.2	1776432	0.606	0.9	0.606
	3	**317400**	**1786158**	**0.762**	**0.8**	**0.762**
	4	314023.1	1795884	0.814	0.7	0.7
	5	310646.3	1805610	0.866	0.6	0.6
	6	307269.4	1815336	0.917	0.5	0.5
	7	304962.5	1825062	0.952	0.4	0.4
	8	304037.3	1834788	0.967	0.3	0.3
	9	303308.8	1844514	0.978	0.2	0.2
	10	302579.5	1854240	0.989	0.1	0.1
	11	301850.2	1863966	1	0	0

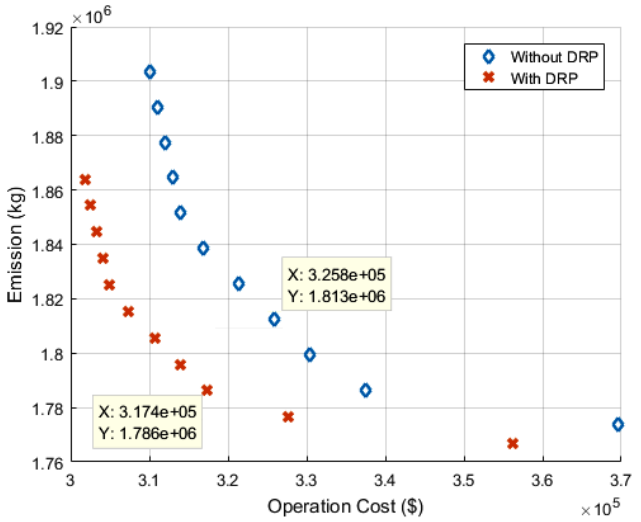

Fig. 8. Pareto front using Epsilon Constraint method in stochastic programming

It is worth mentioning that in the epsilon constraint method, the selected steps are such that ten equal steps are created based on the normalized values of the second constraint (emission). Therefore, the Pareto front includes points that have similar distances to each other. But by using other methods such as Fuzzy Weighted and by using weighting to the objective functions, the method of scattering points can be left to the algorithm itself. Although this does not necessarily lead to a displacement of the Pareto front, it may cause the selection of other points with irregular spacing on the beam front.

Based on Fig. 7, it is evident that, in this case, all points under the utilization of the demand response program are in more favorable conditions compared to the absence of the demand response program. The points located on the Pareto front have both lower costs and lower pollution levels.

Expected Value Programming is a method for analyzing problems with uncertain variables. The focus of this method is on the expected value of the answer.

To perform stochastic programming by minimizing the expected value, wind speed is defined as a random variable, and the expected value of the solution is selected as the objective function. Of course, it should be noted that this answer is still a probabilistic answer, and due to the use of probability distribution, it cannot be considered as a definite answer.

In the second part of the simulation, uncertainty in the wind turbine generating capacity has been considered. By comparing the results with the previous case, it is clear that both operating costs and pollution have increased. The increase in operating costs is 5.34%, and the increase in pollution is 5.4% in the absence of the demand response program. However, in the presence of the demand response program, these increases are 5.38% for operating costs and 5.5% for pollution. Table VII and Fig. 8 present the results of the simulation under uncertainty conditions.

It can be observed that in both cases, incorporating uncertainty into the system in the planning process has

resulted in increased operating costs and pollution. This increase can be interpreted as the cost incurred to enhance the resilience of the planning against the uncertainty of input parameters.

V. CONCLUSION

In this paper, annual energy management in a microgrid consisting of various electrical, thermal, and cooling loads was performed using a multi-objective approach based on the Epsilon Constraint method. Simulation results were obtained considering the presence and absence of demand response in the network, indicating the positive impact of demand response implementation in all scenarios. Furthermore, it was observed that introducing uncertainty in wind speed led to an increase in operating costs by 34.5% and pollution costs by 4.5% in the absence of demand response program, while in the presence of demand response, the increase was 38.5% in operating costs and 5.5% in pollution costs. This increase can be interpreted as the cost incurred for enhancing the resilience of the planning process against input parameter uncertainties. Additionally, since the epsilon constraint method uses fixed steps in the solution process, the Pareto front will consist of points with similar distances, spreading along the middle of the Pareto frontier. It is possible that sufficient concentration in the search space may not occur around the optimal solution. To improve the search process, other optimization methods can be employed to select targeted steps on the Pareto front.

REFERENCES

[1] C. Li, C. Gillum, K. Toupin, Y.H. Park, B. Donaldson, Environmental performance assessment of utility boiler energy conversion systems, Energy Convers. Manag. 120 (2016) 135–143. https://doi.org/10.1016/j.enconman.2016.04.099.

[2] D. Bogdanov, C. Breyer, and North-East Asian Super Grid for 100% renewable energy supply: Optimal mix of energy technologies for electricity, gas and heat supply options, Energy Convers. Manag. 112 (2016) 176–190. https://doi.org/10.1016/j.enconman.2016.01.019.

[3] H. Karami, M.J. Sanjari, H.B. Gooi, G.B. Gharehpetian, J.M. Guerrero, Stochastic analysis of residential micro combined heat and power system, Energy Convers. Manag. 138 (2017) 190–198. https://doi.org/10.1016/j.enconman.2017.01.073.

[4] P. Basak, S. Chowdhury, S.P. Chowdhury, Simscape based modeling and simulation of a PV generator in microgrid scenario, 22nd Int. Conf. Exhib. Electr. Distrib. (CIRED 2013). (2013). https://doi.org/10.1049/cp.2013.1026.

[5] H. Hosseinnia, B. Tousi, Optimal operation of DG-based micro grid (MG) by considering demand response program (DRP), Electr. Power Syst. Res. 167 (2019) 252–260. https://doi.org/10.1016/j.epsr.2018.10.026.

[6] M. Ban, J. Yu, M. Shahidehpour, Y. Yao, Integration of power-to-hydrogen in day-ahead security-constrained unit commitment with high wind penetration, J. Mod. Power Syst. Clean Energy. 5 (2017) 337–349. https://doi.org/10.1007/s40565-017-0277-0.

[7] Y. Maniyali, A. Almansoori, M. Fowler, A. Elkamel, Energy Hub Based on Nuclear Energy and Hydrogen Energy Storage, Ind. Eng. Chem. Res. 52 (2013) 7470–7481. https://doi.org/10.1021/ie302161n.

[8] F. Syed, M. Fowler, D. Wan, Y. Maniyali, An energy demand model for a fleet of plug-in fuel cell vehicles and commercial building interfaced with a clean energy hub, Int. J. Hydrogen Energy. 35 (2010) 5154–5163. https://doi.org/10.1016/j.ijhydene.2009.08.089.

[9] A. Safdarian, M. Fotuhi-Firuzabad, F. Aminifar, M. Lehtonen, A new formulation for power system reliability assessment with AC constraints, Int. J. Electr. Power Energy Syst. 56 (2014) 298–306. https://doi.org/10.1016/j.ijepes.2013.11.027.

[10] A. Zlotnik, L. Roald, S. Backhaus, M. Chertkov, G. Andersson, Coordinated Scheduling for Interdependent Electric Power and Natural Gas Infrastructures, IEEE Trans. Power Syst. 32 (2017) 600–610. https://doi.org/10.1109/tpwrs.2016.2545522.

[11] T. Li, M. Eremia, M. Shahidehpour, Interdependency of Natural Gas Network and Power System Security, IEEE Trans. Power Syst. 23 (2008) 1817–1824. https://doi.org/10.1109/tpwrs.2008.2004739.

[12] C. Shao, X. Wang, M. Shahidehpour, X. Wang, B. Wang, An MILP-Based Optimal Power Flow in Multicarrier Energy Systems, IEEE Trans. Sustain. Energy. 8 (2017) 239–248. https://doi.org/10.1109/tste.2016.2595486.

[13] S.D. Beigvand, H. Abdi, M. La Scala, Economic dispatch of multiple energy carriers, Energy. 138 (2017) 861–872. https://doi.org/10.1016/j.energy.2017.07.108.

[14] M. Salimi, H. Ghasemi, M. Adelpour, S. Vaez-ZAdeh, Optimal planning of energy hubs in interconnected energy systems: a case study for natural gas and electricity, IET Gener. Transm. Distrib. 9 (2015) 695–707. https://doi.org/10.1049/iet-gtd.2014.0607.

[15] A. Shahmohammadi, M. Moradi-Dalvand, H. Ghasemi, M.S. Ghazizadeh, Optimal Design of Multicarrier Energy Systems Considering Reliability Constraints, IEEE Trans. Power Deliv. 30 (2015) 878–886. https://doi.org/10.1109/tpwrd.2014.2365491.

[16] M. Rastegar, M. Fotuhi-Firuzabad, M. Lehtonen, Home load management in a residential energy hub, Electr. Power Syst. Res. 119 (2015) 322–328. https://doi.org/10.1016/j.epsr.2014.10.011.

[17] C. Unsihuay-Vila, J.W. Marangon-Lima, A.C.Z. de Souza, I.J. Perez-Arriaga, P.P. Balestrassi, A Model to Long-Term, Multiarea, Multistage, and Integrated Expansion Planning of Electricity and Natural Gas Systems, IEEE Trans. Power Syst. 25 (2010) 1154–1168. https://doi.org/10.1109/tpwrs.2009.2036797.

[18] S. Pazouki, M.-R.R. Haghifam, Optimal planning and scheduling of energy hub in presence of wind, storage and demand response under uncertainty, 80 (2016) 219–239. https://doi.org/10.1016/j.ijepes.2016.01.044.

[19] M. Yazdani-Damavandi, M.P. Moghaddam, M.-R. Haghifam, M. Shafie-khah, J.P.S. Catalao, Modeling Operational Behavior of Plug-in Electric Vehicles' Parking Lot in Multienergy Systems, IEEE Trans. Smart Grid. 7 (2016) 124–135. https://doi.org/10.1109/tsg.2015.2404892.

[20] A. Parisio, C. Del Vecchio, A. Vaccaro, A robust optimization approach to energy hub management, Int. J. Electr. Power Energy Syst. 42 (2012) 98–104. https://doi.org/10.1016/j.ijepes.2012.03.015.

[21] M.J. Vahid-Pakdel, S. Nojavan, B. Mohammadi-ivatloo, K. Zare, Stochastic optimization of energy hub operation with consideration of thermal energy market and demand response, Energy Convers. Manag. 145 (2017) 117–128. https://doi.org/10.1016/j.enconman.2017.04.074.